Mechanism for spurious structures in photoionization calculations in the independent-particle approximation

Bin Zhou* and R. H. Pratt
Department of Physics and Astronomy, University of Pittsburgh, Pittsburgh, Pennsylvania 15260
(Received 23 September 1991; revised manuscript received 13 January 1992)

A mechanism of unphysical structures in photoionization cross sections calculated in the independent-particle approximation (IPA) has been identified, in a study of the nature of near-threshold structures in the energy dependence of the krypton $3p$ photoionization, generated in the Hartree-Fock-Slater-Latter approximation. We find that overscreening of the IPA potential due to the incomplete cancellation of the electron self-Coulombic interaction and the electron self-exchange interaction in the IPA can lead to a spurious positive barrier in the effective central potential $V_{\rm eff}=V+l(l+1)/2r^2$ for a continuum electron and a consequent spurious shape-resonance-like structure, such as the structure at about 8 eV above the threshold seen in the Kr $3p$ photoionization cross section.

PACS number(s): 32.80.Fb, 32.80.Hd, 32.70.Cs

I. INTRODUCTION

Recently unphysical aspects of the independent-particle (or electron) approximation (IPA) in photoionization calculations, especially for the Hartree-Fock-Slater-Latter model (HFSL), have been discussed, with special attention on the energy dependence of cross sections near but above inner-shell thresholds [1–4]. The motive is to identify features of the calculations that are not artifacts and should be observable. It has been shown that the discontinuity in the derivatives of IPA potentials, introduced at the switch point to a Latter-tail potential, can lead to unphysical oscillatory structures in the cross section. Here we wish to report another kind of unphysical structure, which is of a shape-resonance character and can be produced by overscreening in an IPA potential.

In a recent paper[5] Shanthi, Deshmukh, and Manson performed calculations for the krypton $3p$ partial photoionization cross section at different levels of approximation, such as the HFSL model, the Hartree-Fock (HF) model, and the relativistic random-phase approximation (RRPA), concluding that near-threshold structures found in the partial cross section as a function of photon energy are not due to shape resonances or Cooper minima, and also that they have a physical basis and are not artifacts of the calculation (since in appearance there was a correspondence with structures obtained from approximations beyond the IPA). Here we want to examine in detail these structures seen in the Kr $3p$ photoionization cross section calculated from the HFSL model, trying to understand exactly how in this model they come about. To this end, we employ several other IPA potential models that differ from the HFSL in various ways to see how the observed structures depend on features of the potential. We will conclude, contrary to Ref. [5], that in the Kr $3p$ photoionization cross section calculated with the HFSL potential (Fig. 1), the second maximum at about 100 eV above threshold represents the rise from a zero (Cooper minimum) below threshold; the first maximum, at 8 eV, which only exists in the HFSL model, is a shape-resonance-like peak, reflecting the fact that there is a small positive barrier in the effective central potential seen by the outgoing photoelectron. This positive barrier is a result of the overscreening near the Latter-tail switch point of the HFSL potential, originated from the incomplete cancellation of the electron self-Coulombic interaction and the electron self-exchange interaction. This reveals another way through which artifacts can be generated in near-threshold photoionization cross sections of outer and intermediate subshells in the HFSL calculation and other IPA models. We suggest a rather different origin for the rather different structures seen in calculations beyond the IPA.

It should be noted that, as a model study, our calculations here are only intended to identify features associated with the HFSL model, which has been extensively used in photoionization calculations in the past. We are not discussing the actual threshold behavior, for which electron correlation and relaxation effects not considered in IPA models can be very important, and may lead to physical structures. In Sec. II we will describe the nonrelativistic photoionization theory in the IPA. This will be used in the discussion of krypton $3p$ photoionization in Sec. III. A brief summary will be given in Sec. IV. The atomic units $\hbar=m_e=e=1$ will be used.

II. THEORY

Although our calculations are relativistic and beyond the dipole approximation, we will confine our expository discussion to the nonrelativistic dipole theory, since the nonrelativistic dipole theory can as well explain most features present in our calculations (which are relativistic) here but is much simpler and more intuitive in expression. We review some familiar ideas because they prove to lie at the heart of the spurious features in $V_{\rm eff}$, and also in cross sections, which result from a localization assumption about the exchange potential $U_{\rm ex}$. Neglecting configuration interactions, thereby assuming

atoms are in the lowest-energy configuration, an atomic system of N electrons with nuclear charge Z is described by the HF equations [6]

$$\left[-\frac{1}{2}\nabla_1^2-\frac{Z}{r_1}+V_c(\mathbf{r}_1)\right]u_i(\mathbf{r}_1)-U_{\rm ex}(i,\mathbf{r}_1) =\varepsilon_i u_i(\mathbf{r}_1)\ , \quad i=1,\ldots,N \tag{1}$$

where $u_i(\mathbf{r})$ is the wave function of the ith electron with binding energy ε_i, $V_c(\mathbf{r})$ is the electron Coulombic interaction

$$V_c(\mathbf{r}_1)=\sum_{j=1}^{N}\int d^3\mathbf{r}_2\frac{|u_j(\mathbf{r}_2)|^2}{r_{12}}\ , \tag{2}$$

and $U_{\rm ex}(i,\mathbf{r})$ is the electron exchange interaction

$$U_{\rm ex}(i,\mathbf{r}_1)=\sum_{j=1}^{N}\delta(m_{si},m_{sj}) \times\left[\int d^3\mathbf{r}_2\frac{u_j^*(\mathbf{r}_2)u_i(\mathbf{r}_2)}{r_{12}}\right]u_j(\mathbf{r}_1)\ , \tag{3}$$

with m_s the electron-spin quantum number. Notice the sum on j in V_c and $U_{\rm ex}$ includes all electrons in the atom. Actually the sum should exclude the ith electron since the electron should not interact with itself. But in both $V_c u_i$ and $U_{\rm ex}$ the $j=i$ terms are identical and therefore will cancel each other in the HF equations. In the central-field IPA, the nonlocal exchange interaction $U_{\rm ex}$ expressed in (3) is localized. One writes

$$U_{\rm ex}(i,\mathbf{r}_1)=V_{\rm ex}(r_1)u_1(\mathbf{r}_1)=\gamma\left[\frac{3}{\pi}\rho(r_1)\right]^{1/3}u_i(\mathbf{r}_1)\ , \tag{4}$$

where $\rho(r)$ is the total-electron charge density. In the Kohn-Sham approximation, the exchange coefficient $\gamma=\frac{2}{3}$, while in the Slater approximation $\gamma=1$. Now the Hartree-Fock equations become (assuming $\gamma=1$ is chosen)

$$[-\tfrac{1}{2}\nabla^2-V(r)]u_i(\mathbf{r})=\varepsilon_i u_i(\mathbf{r})\ , \quad i=1,\ldots,N \tag{5}$$

with the localized Hartree-Fock-Slater-Latter potential

$$V(r)=\begin{cases}\dfrac{Z}{r}-V_c(r)+V_{\rm ex}(r) & \text{if } r<r_0\\ \dfrac{Z-N+1}{r} & \text{if } r\geq r_0\ ,\end{cases} \tag{6}$$

where r_0 is the switch point at which the Hartree-Fock-Slater (HFS) potential is just equal to $(Z-N+1)/r$. The Latter-tail potential $(Z-N+1)/r$ was imposed at r_0 to remedy the incorrect asymptotic HFS potential at large distances caused by $V_{\rm ex}\to 0$ when $r\to\infty$. (We will later discuss some other ways to obtain the correct asymptotic potential, such as the vacancy potential.)

The radial HFSL equation is obtained once the wave function is separated into a radial and angular parts. The characteristics of the effective radial potential $V_{\rm eff}[=-V+l(l+1)/2r^2]$ are determined by the interplay of the potential $V(r)$ and the centrifugal potential $l(l+1)/2r^2$. An interesting situation exists for intermediate l (such as $l=3,4$), where $V_{\rm eff}$ may have a double-well structure, with a positive "barrier" between the inner and outer wells, which can cause a shape resonance in the cross section [7].

Near the origin the radial part of the continuum wave function $P_{\varepsilon l'}$ (ε is the kinetic energy of the photoelectron) behaves as $r^{l'+1}$ since the central potential will be large compared to ε. We may write the continuum wave function $P=C\bar{P}$, where $\lim_{r\to 0}\bar{P}_{\varepsilon,l\pm1}=r^{l\pm1}$, and $C_{l\pm1}$ is determined by the normalization condition [8].

The photoionization cross section from an electron in subshell nl within the dipole approximation is proportional to the square of the transition matrix element $R_{\varepsilon,l\pm1}$, given by

$$R_{\varepsilon,l\pm1}=C_{l\pm1}(\varepsilon)\bar{R}_{\varepsilon,l\pm1} =C_{l\pm1}(\varepsilon)\int_0^\infty P_{nl}(r)r\bar{P}_{\varepsilon,l\pm1}(r)dr\ , \tag{7}$$

where $P_{nl}(r),P_{\varepsilon,l\pm1}(r)$ are radial parts of initial and final wave functions of the electron, satisfying the radial HFSL equation.

It should be emphasized that for small ε (near threshold), $\bar{P}_{\varepsilon,l\pm1}(r)$ is relatively independent of ε in the interaction region, which is defined as the region where the matrix element Eq. (7) is largely determined, a region normally confined by the bound-state wave function when ε is smaller than the bound-state binding energy. On the other hand, the normalization factor $C_{l\pm1}(\varepsilon)$, which is determined by $\varepsilon-V_{\rm eff}(r)$ over all distances, can vary sensitively as a function of ε. The rapid variation of $C_{l\pm1}$ with energy can lead to variations in the transition matrix elements and hence the cross section. In the special situation where there is a positive barrier in the effective potential $V_{\rm eff}=l'(l'+1)/2r^2$ of the final wave function $P_{\varepsilon,l'}$, a resonance state may exist above zero energy and $C_{l'}(\varepsilon)$ will exhibit a great enhancement at the resonance energy. As a result, a sharp peak structure, called a shape resonance, appears in the cross section σ_{nl} at this energy [9,10].

The continuum wave functions $\bar{P}_{\varepsilon,l\pm1}$, increasing from the origin with $r^{l\pm1}$, are oscillating functions of r at large distances. Since the matrix element $\bar{R}_{\varepsilon,l\pm1}$ is obtained by an integration over a function $rP_{nl}(r)$ that is independent of energy and a rapidly oscillating function $\bar{P}_{\varepsilon,l\pm1}$, at a certain energy the matrix element may vanish due to complete cancellation of positive and negative portions of the integrand. If this happens in $R_{\varepsilon,l+1}$ for the major contributing channel, a minimum (a Cooper minimum) will be present in σ_{nl} [9–12].

III. CALCULATIONS AND DISCUSSIONS

The partial photoionization cross sections from the Kr $3p$ subshell obtained using the HFSL potential are shown in Fig. 1. There are two local maxima in the cross section, one at about 8 eV and the other at 100 eV of photoelectron energy. Of the two major transition channels $3p\to\varepsilon s,\varepsilon d$, the contribution from $3p\to\varepsilon d$ is much larger and contains both of the structures while the contribution from $3p\to\varepsilon s$ decreases monotonically with energy. The

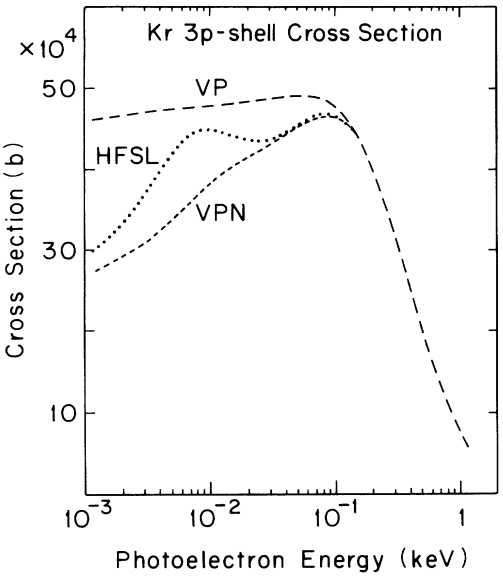

FIG. 1. Photoionization cross sections for the Kr $3p$ subshell obtained using different IPA models: the HFSL model (the dotted curve); the VP model (the long-dashed curve); the VPN model (the short-dashed curve).

question is: what are the natures of these two structures?

From previous work on the distribution of Cooper minima (CM's) [12], we anticipate a CM below threshold in the partial cross section of $3p \rightarrow \varepsilon d$ photoionization (i.e., in the spectrum of photoexcitations) for elements near Kr, which has atomic number $Z=36$; the position of the CM tends to move towards the threshold as Z decreases. A CM below threshold can cause the photoionization cross section to rise from the threshold before decreasing at higher photon energies. We study the plausibility of the existence of a CM by calculating the partial cross sections for $3p$ ionization of elements from $z=30$ to 38, using the HFSL model. We find that the second, higher energy, maximum in the $3p$ partial cross section of Kr also exists in all other nearby elements and as Z decreases the peak shifts towards higher energy. This agrees with a motion of the CM towards threshold from below with smaller Z. By zinc ($Z=30$) the CM shows up above threshold in the $3p$ partial cross section, and the energy interval between the CM and its turnaround peak is about 130 eV. This strongly suggests that the high-energy maximum in the Kr $3p$ partial cross section is the consequence of a CM below the threshold. We have checked the reduced matrix element $\bar{R}_{\varepsilon,l+1}$ for the Kr $3p \rightarrow \varepsilon d$ transition (the contribution of $3p \rightarrow \varepsilon s$ to the $3p$ partial cross section is much smaller) and found that this maximum structure is in $\bar{R}_{\varepsilon,l+1}$, not in the normalization factor $C_{l+1}(\varepsilon)$, as would be expected for a shape resonance. We conclude that the maximum at 100 eV in the Kr $3p$ partial cross section is the manifestation of the superposition of a rise from a CM below the threshold and a hydrogenlike monotonic decreasing behavior at higher photoelectron energy. We note that in a more recent paper Shanthi, Deshmulkh, and Manson also indicated the existence of a CM below threshold for the $3p \rightarrow \varepsilon d$ transition channel of Kr [13].

In order to understand the origin of the first maximum, at 8 eV above the threshold, in the partial cross section of Kr $3p$ photoionization calculated using the HFSL model, we have used several different kinds of IPA models. As various authors have pointed out [2–4] that the discontinuity of the first derivative of the HFSL potential at the switch point may cause oscillations in cross section near threshold, we first used the HFSL potential but with the near-switch-point region locally smoothed by cubic spline interpolation, so that no discontinuity through the second-order derivatives exists anywhere. But the cross section calculated using this smoothed potential is almost exactly the same as before. This indicates in this particular case, *local* smoothing near the switch point has little effect on the structure of the cross section; the discontinuity is not responsible for the appearance of the first peak in the Kr $3p$ cross section of the HFSL model.

Next we compare cross sections produced by two other IPA potentials which do not need to impose the Latter tail: (1) the vacancy potential (VP) in which one of the $3p$ electrons is removed from V_c in the self-consistent calculation; (2) the vacancy potential but with no exchange interactions among electrons (VPN), i.e., $U_{\rm ex}=V_{\rm ex}=0$. Since $V_{\rm ex}$ goes to zero with the total-electron density $\rho(r)$ in the VP as r increases, and the asymptotic form of V_c is $(N-1)/r$ (there are $N-1$ electrons now), the correct asymptotic potential form $(Z-N+1)/r$ will be automatically obtained at large distances, in both the VP and VPN potentials, without any discontinuities in the derivatives of the potential. The Kr $3p$ photoionization cross sections obtained using these two potentials are also shown in Fig. 1. Partial cross sections for both VP and VPN have the maximum at 100 eV above threshold, but neither of them shows the peak at 8 eV. To answer why only the HFSL model has the small peak at 8 eV we have to take a close look at the effective central potentials, shown in Fig. 2 for the major channel $3p \rightarrow \varepsilon d$. In the effective central potential all models have a deep negative well, but only the HFSL model shows a very small barrier

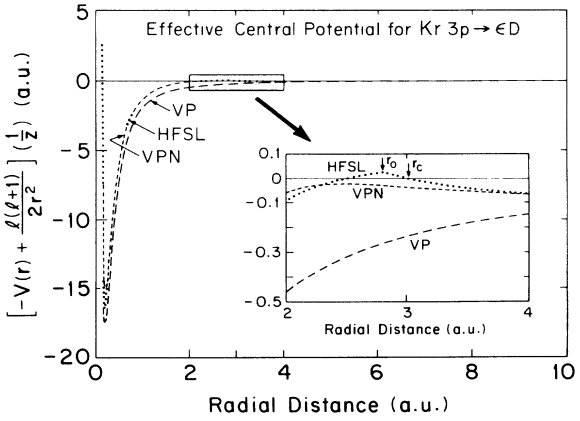

FIG. 2. The effective central potential $[V_{\rm eff}(r)](1/Z)$ of Kr seen by a εd electron in different IPA models: the HFSL model (the dotted curve); the VP model (the long-dashed curve); the VPN model (the short-dashed curve). The inset shows details near the switch point r_0 for the Latter tail in the HFSL potential; r_c is the critical point for $l=2$ (εd electron).

above zero. To see how this barrier affects the continuum wave function we calculate the normalization factor $C_d(\varepsilon)$ of the εd continuum wave function as a function of photoelectron energy ε. After scaling out the normalization function of the hydrogen atom, which we know is a smooth monotonically decreasing function of energy, we find there is a peak in $C_d(\varepsilon)$ at 8 eV in the HFSL model, in agreement with Dillon and Inokuti [14]. For other models no such structure is observed. This indicates that because of the positive barrier in the effective central potential the amplitude of the continuum wave function in the HFSL model has been increased near the origin for energies near 8 eV, in the same sense as for a shape resonance. But in this case the barrier is so low and thin that we do not see the swift change in the phase shift of the continuum wave function, which is usually seen in a shape resonance. And what we see is just a small bump in the cross section instead of a conspicuous sharp dominant peak. We may call this local maximum a quasi-shape-resonance.

But why does only the HFSL model give a positive barrier in the effective central potential? Let us now look at the reduced potential $rV(r)$ of the HFSL, VP, and VPN models, shown in Fig. 3. The potential of the VPN model is close to that of the HFSL model while the potential of the VP model is considerably higher than others. In the VP model, because one of the $3p$ electrons is removed from the shell in the self-consistent calculation [in other words, the self-Coulombic interaction $j=i$ term is excluded from the sum of $V_c(r)$ in (2)] the potential will automatically take the correct Coulombic form at large distances and no tail needs to be imposed. But, remembering that this term is supposed to be canceled by the identical self-exchange term in U_{ex}, removing the electron from the atom means that the exchange interaction is overcounted, which is why the VP potential is

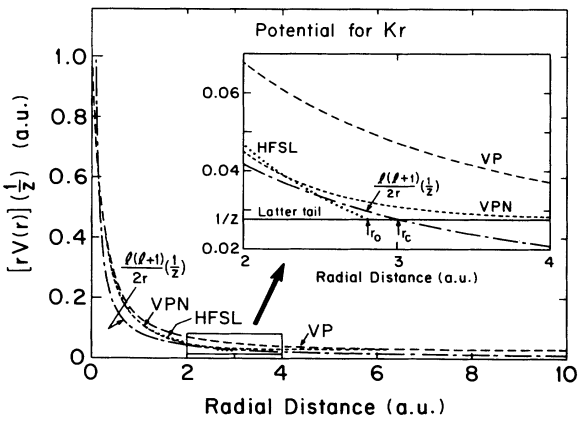

FIG. 3. The reduced potential $[rV(r)](1/Z)$ of Kr in different IPA models: the HFSL model (the dotted curve); the VP model (the long-dashed curve); the VPN model (the short-dashed curve). The inset shows details near the switch point r_0 for the Latter tail in the HFSL potential; also shown are the reduced Latter-tail potential $1/Z$ (the solid line), and the reduced centrifugal potential $[l(l+1)/2r](1/Z)$ of $l=2$ (the long-dashed–short-dashed line); r_c is the critical point for $l=2$ (εd electron).

significantly higher than the others. In the VPN model the exchange interaction is completely omitted ($U_{ex}=0$) in addition to the removal of a $3p$ electron. The correct asymptotic potential is again obtained automatically, as in the VP model. Since the whole exchange interaction is omitted, the problem of overcounting the exchange interaction in the VP model now becomes a problem of undercounting in the VPN model. Certainly a more realistic potential should be between the VP and VPN potentials. When the "real" exchange interaction (excluding the self-exchange term of $i=j$ in the summation) in Eq. (3) is relatively small, the VPN is not a bad approximation to the realistic situation. This may be true for large distances where the real exchange interaction is weak.

In the HFSL model, which uses the localized Slater exchange potential V_{ex} to approximate U_{ex}, the cancellation between the counter terms (the $j=i$ term) in V_c and U_{ex} (eventually V_{ex}) is a crucial problem. Near the origin the cancellation is rather complete because of the large electron density in the region, but at large distance the localized Slater exchange potential V_{ex} drops to zero rapidly with the total-electron density $\rho(r)$, so does the self-exchange interaction $j=i$ term in U_{ex}; the cancellation is not achieved, and the self-Coulombic interaction (the $j=i$ term in V_c) is not completely excluded [15]. This means that the potential is overscreened (overcounting the electron Coulombic interaction) at large distances (at least before r_0) in the HFSL model. Indeed because of the overscreening, the potential of the HFSL model near the switch point drops more steeply than the realistic potential and both VP and VPN potentials as r gets larger. Referring to Fig. 3, this steep drop causes the HFSL potential $V(r)$ near the switch point r_0 to be smaller than the centrifugal potential $l(l+1)/2r^2$ of $l=2$, which is also shown in the inset of the figure, and consequently causes r_0 to be closer to the origin than the critical distance r_c of the εd photoelectron [16]. Since there is a negative inner well in V_{eff} of the εd electron, the result that $r_0 < r_c$ means that there is a positive barrier before r_c in the effective central potential of the εd channel (see Fig. 2). This leads to the small shape-resonance-like structure at about 8 eV in the major channel $3p \rightarrow \varepsilon d$, as seen in the cross section (Fig. 1) [17].

As mentioned earlier, a realistic potential should lie between the potential of VP and that of VPN and hence should be always greater than the centrifugal potential for r near r_0 and larger, as we can see from Fig. 3. Subsequently no positive barrier should exist in the realistic effective central potential. So we see that the overscreening at large distances, caused by the incomplete cancellation of the self-Coulombic interaction with the self-exchange interaction in the localized potential of the HFSL model, gives rise to the first peak at 8 eV in the Kr $3p$ subshell photoionization cross section by producing a small positive barrier in the effective central potential of the continuum electron. The local smoothing near the switch point does not have much effect on the cross section, since the positive barrier due to overscreening still exists and the only effect of the local smoothing is to make the barrier smoother at the switch point. Nevertheless it is possible, as one can easily see from Figs. 2

and 3, that a smoothing over a more extended region near the switch point may make the positive barrier disappear in the effective central potential, considering that the barrier is very small.

It may also be noted that the partial cross section in the VP model has a higher threshold value because the atom in this case is contracted more, due to less screening of the nuclear interaction. Likewise, the threshold value of the VPN model is less than in both the HFSL and the VP models.

In the calculations of the Kr $3p$ subshell photoionization cross section beyond the IPA, a steep drop from the threshold value is observed, followed by a local minimum (see Fig. 1 in Ref. [5]), which is rather different from the structure we just discussed for the IPA level. We suggest this may result from destructive interference between the direct one-electron photoabsorption amplitude, which has a CM below threshold, and the two-electron correlation amplitudes, shifting the CM above threshold, in a similar way as seen in the subshell photoionization cross section of argon $3s$, due there to the strong coupling between $3s$ and $3p$ electrons [18]. Here, however, since the same feature also exists in the HF Kr $3p$ calculation, it seems more likely that the amplitude corresponding to the correlation between the ionic core and the continuum electron, which is present in both the RRPA and HF calculations [5], is responsible for the interference.

IV. CONCLUSIONS

To conclude, calculations with variants of the HFSL model on the Kr $3p$ photoionization have been performed; the structures near the threshold obtained in the HFSL model may be understood in detail. The first peak of the double-peak structure is caused by overscreening at large distances, a defect of the HFSL potential; the second peak is caused by a CM below the threshold. Unlike for the oscillatory structures generated by the discontinuity of the potential derivatives, observed in inner-shell photoionization, the structure generated by the overscreening of the potential is more like a shape resonance in nature and therefore is more likely to appear for subshells of intermediate angular momentum l. The overscreening at large distances is not only a problem for the HFSL model but a genuine defect of IPA models using localized exchange potentials. Considering the numerous calculations based on the HFSL model and other IPA models, one clearly should be very cautious in interpreting the near-threshold structures of photoionization they predict.

*Present address: Department of Physics, Kansas State University, Manhattan, KS 66506.

[1] S. T. Manson and M. Inokuti, J. Phys. B **13**, L323 (1980).
[2] J. Tulkki and T. Aberg, J. Phys. B **18**, L489 (1985).
[3] M. Ya Amusia, I. M. Band, V. K. Ivandov, V. A. Kupchenko, and M. B. Trzhashovskaya, Iz. Akad. Nauk SSSR **50**, 1267 (1986).
[4] Y. Kuang, R. H. Pratt, Y. J. Wu, J. Stein, I. B. Goldberg, and A. Ron, J. Phys. (Paris) Colloq. **48**, C9-527 (1987).
[5] N. Shanthi, P. C. Deshmukh, and S. T. Manson, Phys. Rev. A **37**, 1773 (1988).
[6] H. A. Bethe, *Intermediate Quantum Mechanics* (Benjamin, New York, 1964).
[7] J. Bae, S. H. Kim, J. H. Choi, S. D. Oh, and Y. S. Kim, J. Korean Phys. Soc. **22**, 129 (1989).
[8] H. A. Bethe and E. E. Salpeter, *Quantum Mechanics of One- and Two-Electron Atoms* (Plenum, New York, 1977).
[9] U. Fano and J. W. Cooper, Rev. Mod. Phys. **40**, 441 (1968).
[10] S. T. Manson and J. W. Cooper, Phys. Rev. **165**, 126 (1967).
[11] J. W. Cooper, Phys. Rev. **128**, 681 (1962).
[12] R. Y. Yin and R. H. Pratt, Phys. Rev. A **35**, 1149 (1986).
[13] N. Shanthi, P. C. Deshmukh, and S. T. Manson, Phys. Rev. A **37**, 4720 (1988).
[14] M. A. Dillon and M. Inokuti, J. Chem. Phys. **82**, 4415 (1985).
[15] This is precisely why the Hartree-Slater potential does not have the correct large distance behavior; in this sense, the Latter tail is used to enforce the cancellation at larger distances.
[16] It can be easily shown, from Fig. 3 and Eq. (6), that for the lth partial-wave photoelectron there exists a distance $r_c=[l(l+1)]/[2(Z-N+1)]$ in a.u., at which the effective central potential V_{eff} associated with the Latter-tail potential is zero. If the switch to the Latter tail is made before r_c, i.e., $r_0<r_c$, a positive barrier must be present in the effective central potential, provided that there is an inner negative well in V_{eff}. In our specific case here, $l=2$, $Z=N=36$, hence $r_c=3.0$ a.u., but the switch point is at about 2.8 a.u., thus the positive barrier is seen.
[17] Probably due to the similar kind of barrier in the effective potential, the photoionization cross section of the $3p$ subshell in the Kr neighboring atoms, calculated in the HFSL model, also shows the similar shape-resonance-like behavior: there is a very small peak at about 10 eV above threshold for the bromine atom ($Z=35$), and there is a very pronounced drop from the threshold value for the ruthenium atom ($Z=37$).
[18] M. Ya. Amusya and V. K. Ivanov, Usp. Fiz. Nauk **152**, 185 (1987) [Sov. Phys.—Usp. **30**, 449 (1987)].